ACS OMEGA

Open Access

http://pubs.acs.org/journal/acsodf

Article

Electrochemical Leaching of Cobalt from Cobaltite: Box-Behnken Design and Optimization with Response Surface Methodology

Reyixiati Repukaiti, Arindam Mukhopadhyay, Luis A. Diaz, Caleb C. Stetson, Nighat A. Chowdhury, Hongyue Jin, and Meng Shi*

Cite This: *ACS Omega* 2025, 10, 655−664

Read Online

ACCESS | Metrics & More | Article Recommendations | Supporting Information

ABSTRACT: Cobalt, a critical metal, is anticipated to increase in market demand in the next couple of decades, particularly as a battery material used in electric vehicle application. To boost the domestic production of cobalt in the United States, an electrochemical process has been developed to recover cobalt from a cobaltite-rich concentrate and produce cobalt- and arsenic-rich leachate. The leaching efficiency of cobalt was optimized with a response surface methodology by modifying the electrochemical parameters. A series of experiments based on the Box-Behnken design of experiments were carried out using ferric iron as an electrochemically generated oxidant to leach metals from the concentrate. Operating parameters, such as electrochemical cell current, iron/arsenic molar ratio, and anolyte acidity, were optimized for maximum cobalt recovery. A predicted 73% cobalt extraction efficiency can be achieved with the electrochemically assisted leaching method within 24 h. Compared to other leaching methods, such as bioleaching, electrochemically assisted leaching shows a promising alternative for extracting metals from mining concentrates, showing higher efficiency in less time and under mild conditions.

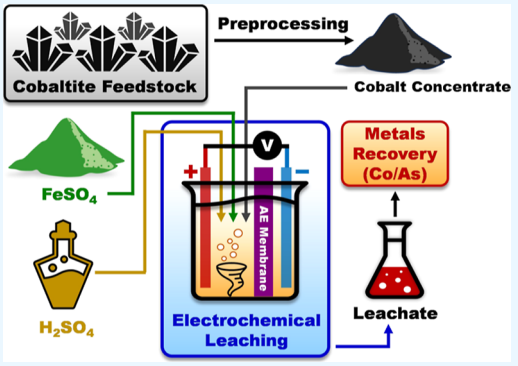

1. INTRODUCTION

As the United States (U.S.) advances the electrification of the energy sector to meet the "net zero carbon" goal by 2050,[1] the demand of critical materials, required for the manufacturing of clean energy storage devices, continues to increase.[2] The growth in electric vehicle manufacturing, which is projected to reach 40% of total passenger car sales in the U.S. by 2030,[3] continues to drive the demand for battery metals, such as lithium (Li), cobalt (Co), nickel (Ni), and manganese (Mn). To establish a more resilient supply chain for these critical metals in the U.S., developments in primary (i.e., mining) and secondary (e.g., recycling of end-of-life products) supplies are urgently needed in this decade. Among these metals, sourcing of Co presents one of the highest supply chain risks.[4] While the global demand for Co is projected to upsurge by up to 15% per year through this decade,[5,6] as much as 70% of Co is currently sourced from the Democratic Republic of the Congo (DRC). This represents a substantial supply risk to several nations, including the U.S. due to their heavy reliance on import and increasing concerns on unsustainable mining practices in DRC.[7,8] To alleviate the impact of potential supply chain disruptions, diversification of Co mining is paramount to ensure the stability of the Co supply chain.[4] Domestic production of Co remains a challenge in the U.S. and requires the deployment of energy-efficient, scalable, economically viable, and environmentally sustainable extraction technologies.

Located in the central region of the state of Idaho, Idaho Cobalt Operations (ICO) contains the largest Co resource (~3.78 million metric tons) in the U.S.,[9] with an average Co grade of 0.52%.[10] The predominant minerals found in the ICO deposits include cobaltite (cobalt arsenic sulfide; CoAsS) and chalcopyrite (copper iron disulfide; $CuFeS_2$).[11] Other notable minerals that are found in minor quantities include pyrite (iron disulfide; FeS_2), pyrrhotite (iron sulfide; FeS), arsenopyrite (iron arsenic sulfide; FeAsS), linnaeite (cobalt nickel tetrasulfide; $(CoNi)_3S_4$), loellingite (iron diarsenide; $FeAs_2$), safflorite (cobalt iron diarsenide; $CoFeAs_2$), enargite (copper arsenic tetrasulfide; Cu_3AsS_4), and marcasite (iron disulfide; FeS_2).[11] Based on the chemical compositions of the mineral deposits, arsenic (As) appears as a major element found at the ICO site, interestingly at higher concentrations than those of Co, iron (Fe), and Cu. The high As content engenders significant challenges for the processing of these ores. Traditional processes, such as roasting, have been established to remove and immobilize As in chemically stable forms.[12] However, release of As, either uncaptured during the roasting

Received: August 14, 2024
Revised: November 28, 2024
Accepted: December 2, 2024
Published: December 23, 2024

https://doi.org/10.1021/acsomega.4c07361
ACS Omega 2025, 10, 655−664

Table 1. Cobalt Leaching Results from Various Feedstocks and Leaching Methods

reference	feedstock	cobalt concentration	method	leaching time	cobalt recovery
Johnson et al.[32]	iron musk ore	1.48%	bioleaching	18 days	50%
Johnson et al.[32]	Bou Azzer concentrate	9.19%	bioleaching	16 days	49%
Abdollahi et al.[31]	cobaltite	1.2%	bioleaching	21 days	92%
Zhang et al.[30]	copper/cobalt-rich sulfide tailings	0.06%	bioleaching	13 days	66%
Ntakamutshi et al.[33]	oxidized copper−cobalt-bearing ore	1.04%	column leaching under reducing condition	7 days	86.72%
Senanayake et al., 2015[24]	smectite ore	0.18%	SO_2 reductive atmospheric H_2SO_4 leaching, 90 °C, 35% pulp density	10 h	97%
Das and De Lange, 2011[25]	nickeliferous smectite ore	0.03%	SO_2/Cu(II) reductive atmospheric H_2SO_4 leaching, 90 °C, 20% pulp density	10 h	97%
Santoro et al.[34]	cobaltiferous ores	<20%	atmospheric H_2SO_4 leach	unknown	80%
Zheng et al.[7]	copper−cobalt sulfide concentrate	6.43%	H_2SO_4 HPAL, P(O_2) = 6 atm, 190 °C, 20% pulp density	2 h	98%
Astuti et al.[35]	nickel laterite ore	0.12%	citric acid leaching, 80 °C, 10% pulp density	5 h	78%
Shen et al.[26]	Ni−Cu−Co matte	2.11%	H_2SO_4 HPAL, P(air) = 1.45 MPa, 150 °C, 20% pulp density	6 h	96%
Kaya et al.[27]	lateritic nickel ore	0.083%	H_2SO_4 HPAL, 255 °C, 30% pulp density	1 h	88%
Zhang et al.[36]	Cu−Co ore	11.58%	ammonium chloride roasting	4 h	90%
Tian et al.[37]	high-Si low-grade Co ore	0.29%	reductive ammonia $(NH_4)_2SO_4$leaching	4 h	95.61%

process or immobilized in unstable products, has severe toxic effects on human health and the terrestrial and aquatic ecosystems and As is, therefore, considered an environmentally regulated metal.[13] Though As can cause severe human health problems and contaminations in water and soil,[14−16] it is still used in medical treatment for tumor therapy[17] and cancer,[18] and catalysts in electroactive film formation[19] and water oxidation.[20]

To develop an efficient Co extraction and As immobilization strategy from the ICO concentrate, relevant literature on extractive metallurgy has been reviewed. Traditionally, Co is recovered as a byproduct from Ni and Cu ores.[21] Approximately, 25% of Co production comes from sulfide ores, for instance, pentlandite (nickel iron cobalt sulfide; $(Ni,Fe,Co)_9S_8$).[21] The general process entails froth flotation to produce a concentrate, smelting to produce sulfide matte, followed by leaching, solvent extraction, and electrowinning to produce Co metal.[22] The smelting process results in a poor Co recovery with a limited efficiency at ∼40%.[21] Another 25% of global Co production comes from Ni laterite ((Fe,Ni)O(OH)) ores. This process begins with high-pressure acid leaching (HPAL), neutralization and counter current decantation to produce sulfide or hydroxide precipitates, which are leached again; the leachate goes through solvent extraction and subsequent Co reduction through electrowinning.[22] As high as 93% Co recovery can be achieved from this process.[21] The remaining 50% of global Co production comes mostly from Cu−Co sulfide ores, such as carrollite (Co_2CuS_4).[21] These ores have similar processing routes as those of Ni sulfide ores, with the addition of an impurity removal step after solvent extraction.[22] Co recovery as high as 62% can be achieved with these strategies.[21]

To further improve the extraction efficiency of Co recovery, various leaching methodologies have been developed in the literature, including reductive leaching, HPAL, and bioleaching. Table 1 compares literature reports on Co recovery from different feedstocks with diverse leaching strategies. Reductive leaching employs reducing agents such as sulfur dioxide (SO_2) to reduce and dissolve high-valent metal oxides.[23] This strategy allows for Co recovery as high as 97% within a relatively short leaching time frame, for example, 10 h.[24,25] HPAL is the most developed and industrially applied approach, allowing for high Co yields (78−98%) within a much shorter leaching time, for example, 6 h.[7,26,27] HPAL, however, is generally operated at high temperatures (∼255 °C) and high O_2 partial pressure (∼1000 kPa) to ensure the oxidation and dissolution of refractory metals from sulfide-based minerals.[7,26−28] Therefore, this method is energy intensive and costly.[29] Bioleaching strategies are an environmentally friendly alternative to traditional hydrometallurgical leaching for the extraction of Co.[30] This strategy harnesses the natural capability of microorganisms to generate oxidizing agents. However, bioleaching processes are usually slow and may require several weeks to achieve modest-to-high (49−92%) Co recovery.[30−32] A low technological readiness level (TRL) and poor economic viability continue to hinder the industrial adoption of bioleaching for efficient Co recovery.

As, one of the main elements in the ICO concentrate (Table S1), is generally bonded with other metals to form arsenates, arsenides, sulfides, and oxides. Some common primary arsenic-bearing minerals are arsenopyrite (FeAsS), cobaltite (CoAsS), enargite (Cu_3AsS_4), gersdorffite (NiAsS), orpiment (As_2S_3), and realgar (AsS).[38−40] In order to extract the valuable metals, such as Co, Ni, and Cu, As needs to be isolated and immobilized in stable forms, which is currently performed utilizing established processing methods.

Pyrometallurgical methods usually involve roasting, converting, and smelting of sulfide ores, and arsenic is captured from electrostatic precipitators or wet gas scrubbers.[39] As is mostly oxidized or sulfurized to As oxides and/or sulfides, such as As_2O_3 and As_2S_3[40]. The captured As containing products could go back to the smelting process or further immobilization process, depending on the economic values. Additional hydrometallurgical processing is aimed to immobilize arsenic in stable forms.[39−41] Generally, autoclave precipitation with high pressure and temperature oxidation are utilized.[41]

Hydrometallurgical processing of As bearing minerals generally involves leaching of the minerals followed by As

https://doi.org/10.1021/acsomega.4c07361
ACS Omega 2025, 10, 655−664

immobilization in a stable form. Depending on the feedstock ores, several leaching procedures have been established, such as alkaline sulfide leach, alkaline hypochlorite leach, high pressure acid oxidation, and bacterial oxidation.[40] After leaching, As is commonly immobilized via precipitation of arsenical ferrihydrite ($5Fe_2O_3{\cdot}9H_2O$) with arsenate absorbed internally, or crystalline scorodite ($FeAsO_4{\cdot}2H_2O$).[40] Both products are required to have less than 5 mg/L As leachability according to the U.S. Environmental Protection Agency's standard.[42]

Electrochemically assisted leaching is a promising strategy for sustainable extractive hydrometallurgy, as electrons obtained from carbon-free energy sources can be employed to promote chemical reactions decreasing the need for chemical reagent intensive processes.[43] In our research group, we have developed electro-hydrometallurgical strategies to recover diverse critical clean energy metals and valuable metals from end-of-life materials, such as electronic wastes and spent lithium-ion batteries.[44−46] Compared to traditional hydrometallurgical routes, electrochemically assisted hydrometallurgical strategies have demonstrated superior economic viability, environmental sustainability, and technological readiness.[47]

In the present study, we proposed and evaluated a novel electrochemically assisted leaching strategy to extract Co from cobaltite-rich concentrates (from ICO operations) at moderate temperature and ambient pressure; cf. Figure 1. This approach

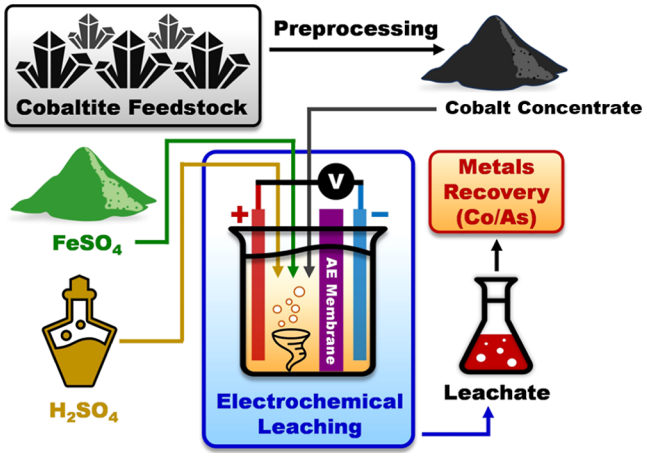

Figure 1. Conceptualization of electrochemically assisted leaching of cobaltite (CoAsS) to recover Co and As.

aims to address some of the limitations of existing leaching strategies relevant to Co recovery by developing a process that operates under ambient conditions with relevant extraction kinetics and yields. The electrochemically assisted leaching strategy presented herein exploits electrons for continuous electrochemical regeneration of the oxidizing agent, ferric iron (Fe^{3+}), to extract Co and As from CoAsS without the requirements of high temperature, high pressure, long leaching timeframes, and high concentrations of redox reagents. Proof of concept was complemented with a Box-Behnken experimental design and response surface methodology (RSM)-based optimization to understand the statistical significance of three main operating factors on the Co extraction efficiency, i.e., current in electrochemically assisted leaching, Fe-to-As molar ratio, and acidity (H_2SO_4 concentration) of the anolyte. Optimization of the electrochemically assisted leaching process to maximize Co extraction efficiency is anticipated to facilitate future efforts to advance the TRL (current TRL = 2) and improve the economic viability of the approach.

2. MATERIALS AND METHODS

2.1. Cobalt Concentrate Material. The cobalt concentrate (i.e., cobaltite-rich feedstock) examined herein was obtained from ICO in central Idaho, U.S. To characterize the chemical composition of the concentrate, the material was digested in aqua regia. Analytical characterization using inductively coupled plasma−optical emission spectroscopy (ICP-OES) revealed that the cobalt concentrate material contained 15.11 wt % As, 12.29 wt % Fe, 9.22 wt % Co, and 1.74 wt % of Cu. Details are provided in Table S1 of the Supporting Information. Additionally, to structurally characterize the solid state of the material, powder X-ray diffraction (XRD) was employed. As shown in Figure S1 of Supporting Information, the XRD profile revealed that the material consisted of various sulfides (FeS, CoAsS, and AsS) and oxides (As_2O_3 and SiO_2). The presence of SiO_2 was expected in the material because quartz is typically found in mining concentrates.[32,48,49]

2.2. Electrochemically Assisted Leaching. A custom-made electrochemical cell with two compartments (anodic and cathodic chambers each with a maximum occupiable volume of 175 mL) was used in the study under air; as seen in Figure S2 in the Supporting Information. The anodic and cathodic chambers were separated with an anion exchange membrane (AGC Chemical Americas, FORBLUE SELEMION). The electrochemistry was carried out in an aqueous medium. The aqueous anolyte held 80 mL of the leachate containing sulfuric acid (H_2SO_4), ferrous sulfate ($FeSO_4$), and 10.589 g of cobalt concentrate (13.23% pulp density). A titanium mesh coated with iridium oxide (IrO_2) was used as the anode (immersed surface area = 10 cm^2). The anolyte acidity was controlled by the molarity of H_2SO_4, and the Fe/As molar ratio was adjusted with the amount of ferrous sulfate in the anolyte. The aqueous catholyte contained 100 mL of 1 M H_2SO_4 solution and a platinum mesh cathode (immersed area = 15 cm^2). In order to simplify data processing, all the reported cell's current values are shown in absolute terms (mA). The anolyte was heated at 70 °C (leaching temperature) using heating mantle tape, while the reaction contents were continuously stirred with an overhead mechanical stirrer (700 rpm) for 24 h.

The progress of the electrochemical process, in each case, was monitored via chronopotentiometry using a BioLogic's potentiostat and the EC-lab software (V11.34). An example of the cell voltage profile is provided in Figure S3 of Supporting Information, which were used to determine electrical energy consumption (kW h). Table S2 of the Supporting Information provides pertinent details.

Following electrochemically assisted leaching, the anolyte was filtered through double P8 (pore size = 20 μm) filter papers to separate the undissolved material and the leachate. The anolyte compartment, anode, and stirrer were rinsed during the filtration process. The volume of the anolyte containing dissolved Co, As, and other metals was measured; the undissolved material was dried at 75 °C in an oven for at least 12 h and weighed. Approximately 125 mg of undissolved material was digested (12 h at room temperature) in 20 mL of aqua regia solution to determine residual Co and As concentrations. The volume of the catholyte was also measured after leaching experiments. Anolyte, catholyte, and the digested solution of undissolved fractions were analyzed by atomic

https://doi.org/10.1021/acsomega.4c07361
ACS Omega 2025, 10, 655−664

absorption spectroscopy (AAS, Agilent 240FS) for Co, Fe, and other metal concentrations, while As concentrations were measured with ICP-OES. Notably, due to minor cation migration through the anion exchange membrane from the anolyte to the catholyte, some leached Co and As contents were also detected in the catholyte. This is due to the large concentration gradient of cations in the two chambers. Hence, the total extraction efficiency (%) for each of the metals was determined by considering the sum of metal mass in both the anolyte and catholyte, as shown in eq 1.

$$\text{Extraction efficiency (\%)} = \left[\frac{m_{\text{anolyte}} + m_{\text{catholyte}}}{m_{\text{feedstock}} \times \text{metal wt \%}}\right] \times 100\% \quad (1)$$

Details of extraction efficiencies of Co and As are provided in Table S2 of Supporting Information.

2.3. Experimental Design and Optimization. This study employed a three-factor and three-level Box-Behnken (BB) response surface design[44] to understand the statistical significance and impact of three process parameters (predictor variables): current (A; unit: mA), Fe/As molar ratio (B), and anolyte H_2SO_4 concentration (C; unit: M), on the Co extraction efficiency (response variable) through the proposed electrochemically assisted leaching of the cobalt concentrate. The levels of the three factors are shown in Table 2, yielding a total of 15 experimental conditions. Applying BB design is rationalized as follows: (1) this design requires the least number of experiments for a three-factor and three-level analysis with equally spaced intervals between the levels and (2) this design precludes factorial combinations at the vertices of the process space, thus alleviating the need to conduct experiments at extreme conditions that may result in high electrode polarization and undesired reactions, such as oxygen and sulfur dioxide evolution.[44] The rationale behind selecting the current values is based on electrochemical leaching work of metal recovery from the lithium-ion battery black mass to maintain current density in the range: 20−50 mA/cm^2.[50,51] For the Fe/As molar ratio values, literature shows a range of Fe/As ratios from 1.5 to 5,[39,52−55] while larger ratios show a higher leaching yield, a sufficient Fe/As ratio is yet to be determined to avoid excessive Fe addition. The acid concentration range from 1 to 2 M is selected due to the low solubility of CoAsS.

Table 2. Operational Values of 3 Different Factors at 3 Different Levels Using Box-Behnken Design

factor	low level: −1	intermediate level: 0	high level: +1
A: cell current	200 mA	350 mA	500 mA
B: Fe/As molar ratio	1.50	3.25	5.00
C: anolyte H_2SO_4 concentration	1.0 M	1.5 M	2.0 M

Analysis of experimental data on the Co extraction efficiency was carried out with Minitab 18. RSM.[44] Statistical analysis was employed to understand the relative influence of the studied factors on the response variable to the overall process, i.e., Co extraction efficiency. Analysis of variance (ANOVA) was used to estimate the statistical significance of the individual factors and their quadratic and 2-way interaction terms on the response variable. While a full second-order regression model was initially developed, backward elimination was performed to remove nonsignificant contributions, reduce the number of variables, and improve the weighted predicted correlation coefficient, R^2. This study revealed optimal conditions to achieve a maximum Co extraction efficiency based on unique combinations of the three experimental factors.

3. RESULTS AND DISCUSSION

3.1. Electrochemically Assisted Leaching. The electrochemically assisted leaching method employs electrons to continuously regenerate the oxidizing agent, Fe^{3+}, thereby leaching Co and As from the cobalt concentrate in an acidic aqueous medium. Leaching of the concentrate occurs within the anodic compartment of the electrochemical cell. As depicted in Figure 2, the process starts with Fe^{3+}-mediated

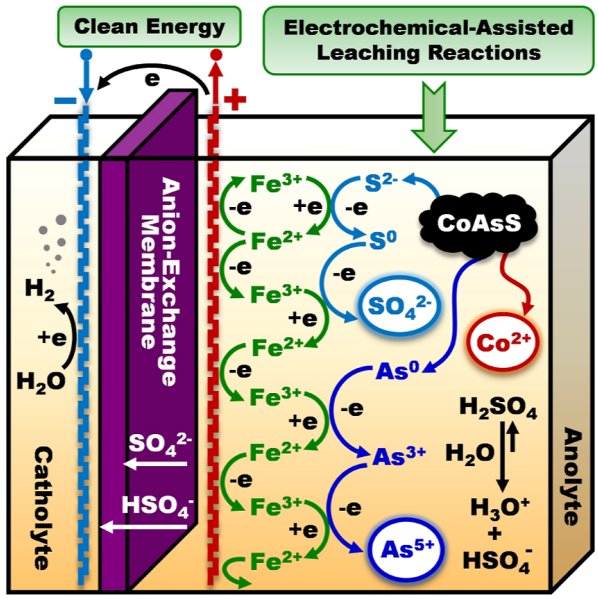

Figure 2. Schematic representation of electrochemically assisted leaching of cobaltite (CoAsS) to recover Co and As. Pertinent redox reactions based on proton-coupled electron transfer and other chemical reactions are demonstrated.

oxidation ($E_{Fe^{3+}/Fe^{2+}} = 0.77$ V NHE)[56] of the sulfide anion (S^{2-}) in CoAsS to elemental sulfur (S^0, $E_{S^0/S^{2-}} = -0.48$ V NHE[56]) and further oxidation to the sulfate anion (SO_4^{2-}, $E_{SO_4^{2-}/S^0} = 0.31$ V NHE[56]); Fe^{3+} undergoes reduction to Fe^{2+} in the process. The oxidation of sulfide results in the liberation of the Co^{2+} cation and elemental As (As^0) from the cobalt concentrate in the aqueous H_2SO_4 medium. Subsequently, Fe^{3+} oxidizes elemental As^0 to its higher valent cationic forms, i.e., As^{3+} ($E_{As^{3+}/As^0} = 0.24$ V NHE[56]) and As^{5+} ($E_{As^{5+}/As^{3+}} = 0.58$ V NHE[56]). Anodic oxidation of Fe^{2+} to Fe^{3+} permits the continuous electrochemical regeneration of Fe^{3+} in the reaction mixture. The balanced redox reactions, as shown in eqs 2−6, are based on the mechanism proposed by Taylor and Vanderloop but replacing the use of oxygen with Fe^{3+} as the electrochemically generated oxidant.[57]

$$\text{CoAsS(s.)} + 2Fe^{3+}(\text{aq.}) \rightarrow Co^{2+}(\text{aq.}) + As^0 + S^0_{(s)} + 2Fe^{2+}(\text{aq.}) \quad (2)$$

https://doi.org/10.1021/acsomega.4c07361
ACS Omega 2025, 10, 655−664

$$As^0 + 3H_2O + 3Fe^{3+}(aq.) \rightarrow H_3AsO_3(aq.) + 3H^+ + 3Fe^{2+}(aq.) \quad (3)$$

$$H_3AsO_3(aq.) + H_2O + 2Fe^{3+}(aq.) \rightarrow H_3AsO_4(aq.) + 2H^+ + 2Fe^{2+}(aq.) \quad (4)$$

$$S^0_{(s)} + 4H_2O + 6Fe^{3+}(aq.) \rightarrow 8H^+ + SO_4^{2-}(aq) + 6Fe^{2+}(aq.) \quad (5)$$

$$Fe^{2+}(aq.) \rightarrow Fe^{3+}(aq.) + e^- \quad (6)$$

In contrast to the anodic processes, the cathodic process involves the hydrogen evolution reaction according to eq 7. To maintain electroneutrality, sulfate (SO_4^{2-}) and bisulfate (HSO_4^-) anions are transferred through the anion-exchange membrane (Figure 2).

$$2H^+ + 2e^- = H_2 \quad (7)$$

3.2. Statistical Significance of Different Operating Factors on the Co Extraction Efficiency.

Table 3 shows the summary of three-factor and three-level BB response surface design for the electrochemically assisted leaching of the Co concentrate. The design consisted of 15 experimental conditions with different combinations of the three factors set at low (−1), intermediate (0), and high (+1) levels. Table 3 and Figure S4 in the Supporting Information show that extraction efficiencies of Co and As are at their lowest values (15% and 18%, respectively) in set 1 while their highest values (57% and 62%, respectively) are in set 4. This shows that the metal extraction efficiency is the highest at the high level (+1) of both the current (A) and Fe/As molar ratio (B). The trend in the extraction efficiency appears to be nearly identical for Co and As, cf. Table 3. It is an expected result due to the co-occurrence of Co and As within the mineral cobaltite and similar leaching kinetics in the cobalt concentrate.

Table 3. Summary of BB Response Surface Design for Electrochemically-Assisted Leaching of Cobalt Concentrate, Showing Different Experimental Sets, Design's Factor Level Combinations, and Pertinent Metal Extraction Efficiencies

set	level of factor			extraction efficiency (%)	
	A: current	B: Fe/As molar ratio	C: anolyte H_2SO_4 conc.	Co	As
1	−1	−1	0	15.42	18.51
2	+1	−1	0	31.85	31.98
3	−1	+1	0	16.52	18.66
4	+1	+1	0	62.07	56.78
5	−1	0	−1	29.08	26.43
6	+1	0	−1	51.58	56.58
7	−1	0	+1	33.18	37.61
8	+1	0	+1	49.75	45.22
9	0	−1	−1	44.71	44.24
10	0	+1	−1	54.45	52.50
11	0	−1	+1	36.49	35.50
12	0	+1	+1	57.34	56.61
13	0	0	0	22.52	28.47
14	0	0	0	33.40	31.57
15	0	0	0	35.65	33.35

Based on the BB design matrix and experimental outcomes, a full second-order quadratic model was developed to account for the variability of the response surface with changes in the factors. Details of the ANOVA results are provided in Tables 4, S3 and S4 of the Supporting Information. While this full model offered good correlation coefficients, R^2 = 94.23% and R^2 (Adj) = 83.84%, it yielded a relatively poor prediction, R^2 (Pred) = 53.27%. To reduce the risk of overfitting, backward elimination was performed by removing non-statistically significant factors or interactions. The quadratic (AA and BB) and 2-way interaction (AC and BC) terms were removed from the full model. By modifying the full model, a reduced second-order quadratic model was developed to yield better R^2 (Pred), 70.43%. Details are provided in Tables 4 and S2 to S4 of the Supporting Information.

Equations 8 and 9 show uncoded regression equations for the full quadratic versus reduced second-order quadratic models, respectively.

$$\text{Co extraction efficiency} = 1.435 + 0.00123A - 0.1885B - 1.671C - 0.000001AA + 0.01354BB + 0.543CC + 0.000277AB - 0.000198AC + 0.0317BC \quad (8)$$

$$\text{Co extraction efficiency} = 1.415 - 0.000059A - 0.0528B - 1.629C + 0.540CC + 0.000277AB \quad (9)$$

The analyses of residuals are depicted in Figures S5−S8. It is evident that the residual terms are normally distributed around zero (i.e., have an expected value of zero) and demonstrate equal variance. Therefore, the regression models can be considered to be valid. Figure 3 presents a pareto chart and a normal plot of statistical significance which allows interpretation of the relative standardized effects and accordingly, the statistical significance of the different factors, quadratic, and 2-way interaction terms on the Co extraction efficiency, i.e., the response variable. It is evident that Co extraction efficiency is most impacted by the individual influence of A (i.e., current) and the least impacted by the individual influence of C (i.e., anolyte H_2SO_4 concentration).

Intriguing effects of three factors and their combined influence (via 2-way interaction) on the response variable (i.e., Co extraction efficiency) can be visualized in the two-dimensional contour plots in Figure 4. These contour plots were developed from the reduced second-order regression model of the response variable. Contour plots of the full-quadratic model of the response variable are shown in Figure S9 in the Supporting Information. In each case, one of the three factors was kept constant at the intermediate level (0), while the other two factors varied within the experimental range from low (−1) to high (+1) levels to observe changes in the response variable. Figure 4A−C depicts two-dimensional changes to the response variable through variations in the 2-way interactions between A and B, A and C, and B and C, respectively. Accordingly, the 2-way interaction between A and B at their high levels (+1) yields a high response (the darkest green area marked within the red triangle). In contrast, Figure 4B,C reveals that a 2-way interaction of A (B) at a high level (+1) with C (C) at either low (−1) or high (+1) levels generates a similar response. This indicates that the 2-way

https://doi.org/10.1021/acsomega.4c07361
ACS Omega 2025, 10, 655−664

Table 4. Details of ANOVA for a Full and Reduced Second-Order Quadratic Models Derived from the BB Design and the Experimental Results, Showing the Statistical Significance of Different Factorial Terms on the Co Extraction Efficiency as the Response Variable

model type	full second-order model				reduced second-order model			
source	DF	contribution	*F*-value	*P*-value	DF	contribution	*F*-value	*P*-value
model	9	94.23%	9.07	0.013	5	89.20%	14.87	0
linear	3	59.13%	17.07	0.005	3	59.13%	16.43	0.001
A	1	42.96%	37.21	0.002	1	42.96%	35.82	0
B	1	16.13%	13.97	0.013	1	16.13%	13.44	0.005
C	1	0.04%	0.03	0.861	1	0.04%	0.03	0.86
square	3	26.63%	7.69	0.025	1	22.94%	19.12	0.002
AA	1	2.51%	1.11	0.341				
BB	1	1.20%	1.85	0.232				
CC	1	22.91%	19.85	0.007	1	22.94%	19.12	0.002
2-way interaction	3	8.47%	2.45	0.179	1	7.14%	5.95	0.037
AB	1	7.14%	6.18	0.055	1	7.14%	5.95	0.037
AC	1	0.30%	0.26	0.634				
BC	1	1.04%	0.9	0.386				
error	5	5.77%			9	10.80%		
lack-of-fit	3	2.45%	0.49	0.723	7	7.48%	0.64	0.724
pure error	2	3.32%			2	3.32%		
total	14	100.00%			14	100.00%		
R^2	94.23%				89.20%			
R^2 (Adj)	83.84%				83.21%			
R^2 (Pred)	53.27%				70.43%			

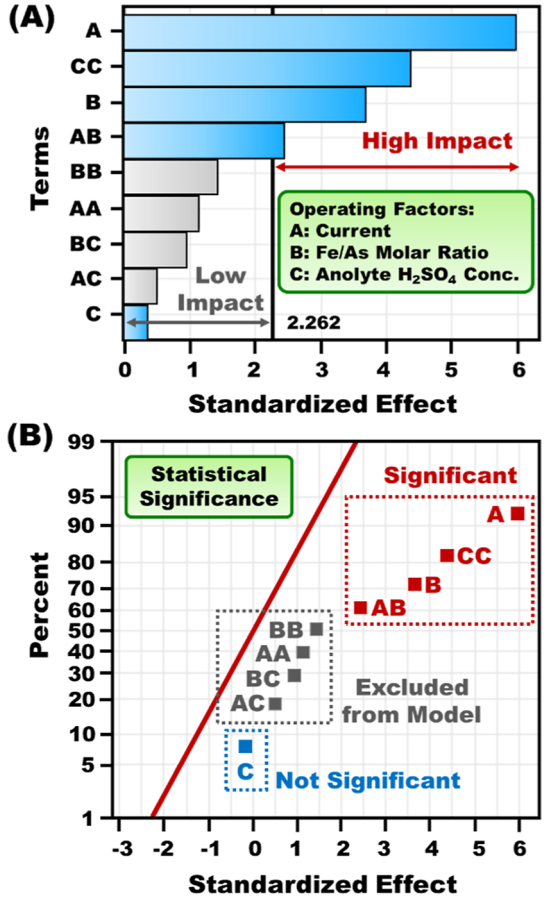

Figure 3. Pareto chart of standardized effects (A) and normal plot of statistical significance (B) for different operating factors, their quadratic and interaction terms on the Co extraction efficiency as the response variable.

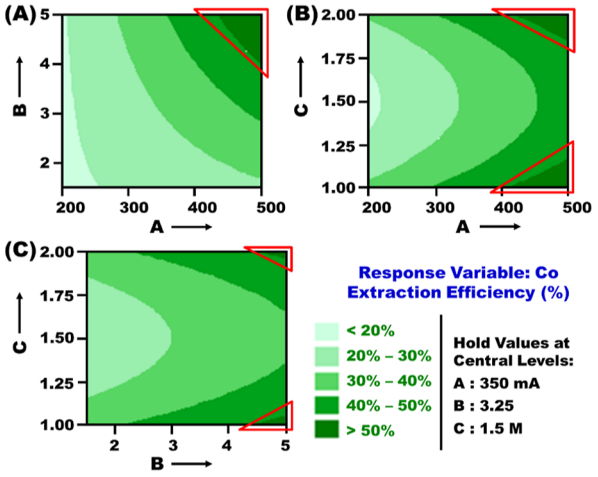

Figure 4. Two-dimensional contour plots depict interactive influences of three operating factors (A, B, and C) on the Co extraction efficiency as the response variable. The darkest green areas within red triangles represent the maximum response.

interaction of A vs B is statistically more significant than that of A vs C and B vs C. The same trends can be observed from the full-quadratic model contour plots in Figure S8.

The above analysis demonstrates that term A (current) has the most significant influence on the Co extraction efficiency. This corroborates that the overall leaching process is primarily driven by electrochemistry. Specifically, increasing current promotes faster redox reactions in the anolyte and hence faster leaching kinetics for the release of Co from the cobalt concentrate in the nonhomogeneous anolyte system. Higher current drives the chemical equilibrium forward by increasing the polarization of the electrodes, thereby facilitating faster electrochemical regeneration of the oxidizing agent, Fe^{3+}. The second most influential factor, B (Fe/As molar ratio), is also

https://doi.org/10.1021/acsomega.4c07361
ACS Omega 2025, 10, 655−664

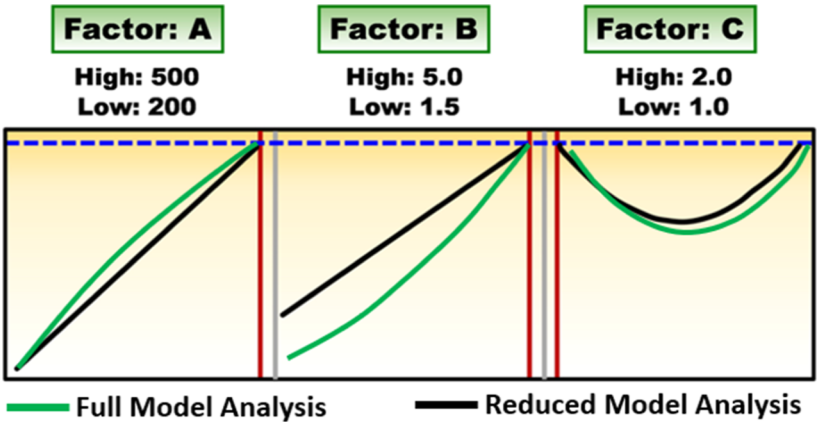

Figure 5. Response surface optimization result from full and reduced model analysis, showing the optimal leaching condition within the design region.

important for improving Co extraction efficiency. This can be rationalized by the higher concentration of the oxidizing agent, Fe^{3+}, driving the equilibrium of the redox reactions in the anolyte to enable faster leaching kinetics according to Le Chatelier's principle. The significance of factors A and B on the Co extraction efficiency is amplified by the statistical importance of their 2-way interaction term AB as mentioned earlier. Factor C (anolyte H_2SO_4 concentration) has the least impact on the Co extraction efficiency. This could be explained by the presence of two competing processes: the cogeneration of SO_4^{2-} anions from the H_2SO_4 and oxidation of CoAsS (oxidation of S^{2-} to S^0, and S^0 to SO_4^{2-} in eqs 2 and 5, respectively). As the concentration of SO_4^{2-} increases during the reaction, the overall equilibrium is driven backward in eq 5; hence, the reaction rate is decreasing according to the Le Chatelier's principle. To sum up, there is an optimal combinatorial balance for three factors to maximize the efficiency of electrochemically assisted extraction of Co.

Figure S10 illustrates the 3D response surface plots, providing an easier visual representation of how the predictor variables affect the response variable. Notably, the extraction efficiency of Co increased from 20% to 60% when both electric current and Fe/As molar ratio grew from their minimum values to the maximum values (i.e., 200 to 500 mA and from 2 to 5, respectively). This suggests the possibility of a better design matrix beyond the current parameter range examined in this study. Additionally, the Co extraction efficiency initially decreased as the anolyte concentration went from 1 to 1.5 M but then began to rise as the acid concentration was further increased, up to 2 M. Because a higher concentration of anolyte H_2SO_4 would lead to higher leaching cost, further exploration may also focus on the anolyte H_2SO_4 concentration lower than 1 M.

3.3. Optimization of the Co Extraction Efficiency. To identify the optimal operational conditions that maximizes the Co extraction efficiency, we sought to employ response surface optimization based on the results in Table 3. The results from both full and reduced models are summarized in Figure 5. The optimal conditions for full model analysis comprise a current of 500 mA, 5:1 molar ratio of Fe to As, and 2 M anolyte H_2SO_4, which would yield a Co extraction efficiency of 73.6% with a desirability of 72.6%. The 95% confidence interval for the Co extraction efficiency ranged from 55% to 91%, whereas the 95% prediction interval was 50%−96%. For the reduced model analysis, the optimal conditions are a current of 500 mA, 5:1 molar ratio of Fe and As, and 1 M of anolyte H_2SO_4. The predicted optimal Co extraction would be 72.6% with a desirability of 60.8%, the 95% confidence interval was from 60% to 84%, and the 95% prediction interval ranged from 54% to 90%. The response surface optimization between the full and reduced models are mostly in agreement, except the factor C of anolyte acidity. Therefore, both optimal conditions were explored in additional experiments.

Based on the optimal parameters from response surface optimization on both full and reduced model analyses, electrochemical leaching experiments were performed at 1 and 2 M of anolyte H_2SO_4, with consistent current of 500 mA and 5:1 molar ratio of Fe to As. The extraction efficiencies of Co are 50% and 33% for full and reduced model analyses, respectively. These Co extraction efficiencies have large discrepancies with the predicted optimal values of 73.6% for full-and 72.6% for reduced model analysis. The optimal parameter experiments were carried out 30 days after the BB design experiments. Even though the anion exchange membrane was conditioned in deionized water, membrane degradation or fouling could have occurred lowering the ion exchange rate between the anolyte and catholyte.[58] Additionally, minor iridium oxide anode degradation (color changing) was also observed during BB experiments, which could cause higher current resistance.[59] Other reasons may include temperature, anode material, and cell design that caused the large discrepancies between the predicted optimal conditions and experimental optimal conditions results.

We surmise that the Co extraction efficiency via electrochemically assisted leaching may depend on several other factors beyond the three operating factors that were thoroughly examined in the present study. With the goal of improving the leaching efficiency of the cobalt concentrate beyond factors A, B, and C, the impact of other parameters on the leaching yield was also considered. As in many extractive metallurgy systems, mass transfer is the primary barrier to leaching of cobalt from the concentrate.[60,61] To improve the mass-transfer efficiency, cell design and anolyte agitation were modified. However, small amounts of cobalt concentrate were observed in restricted spaces within the anolyte compartment, for example, in narrow corners and at the cell meniscus. Generally, increasing the agitation speed improved the leaching yield, with 700 rpm determined to be the highest agitation speed obtainable before the anolyte overflowing from the cell. Temperature also plays an important role in leaching efficiency

https://doi.org/10.1021/acsomega.4c07361
ACS Omega 2025, 10, 655−664

because leaching increases with higher temperatures by reducing the limitations imposed by mass transfer.[62,63] The limiting factor was the maximum working temperature of the anion exchange membrane because it deteriorated at temperatures above 70 °C.[64] Ultimately, the compatibility of hardware must be improved to further increase the efficiency of mass transfer and leaching yield.

4. CONCLUSIONS

In summary, this detailed study focuses on optimization of a novel electrochemically assisted leaching process to recover Co, a critical clean energy metal, and As, an environmentally regulated metal, from a cobalt-rich concentrate. The strategy is based on exploiting electrons to extract Co and As from the cobalt concentrate in the presence of ferrous iron (Fe^{2+}) in an acidic aqueous medium. The study employed a three-factor three-level Box-Behnken experimental design to garner insight into the influence of three major operating factors, (i.e., current, Fe/As molar ratio, and anolyte H_2SO_4 concentration) on the Co extraction efficiency as the response variable. Response surface methodology analyses via development of full and reduced second-order regression models revealed the statistical significance of the operating factors and their quadratic and 2-way interaction terms in modulating the Co extraction efficiency. The response variable showed strong dependencies of metal recovery on current and Fe/As molar ratio. The results reveal the importance of these two factors in facilitating faster redox reaction kinetics and driving forward the overall chemical equilibrium.

Response surface optimization predicted achieving ∼73% Co extraction efficiency with the electrochemically assisted leaching method using both full and reduced model analyses. The full model analysis optimal condition comprised a current (A) = 500 mA, Fe/As molar ratio (B) = 5.0, and anolyte H_2SO_4 concentration (C) = 2.0 M. The reduced model provided a higher R^2 value after eliminating nonsignificant variables, with optimal conditions: current (A) = 500 mA, Fe/As molar ratio (B) = 5.0, and anolyte H_2SO_4 concentration (C) = 1.0 M instead. The importance of the study arises from the method's practical viability, allowing similar or higher Co recovery efficiency as those reported in the literature while decreasing the operational time frame (24 h) as compared to multiple days to weeks. While this work demonstrates a case study for recovering Co from a mining concentrate, we envision the principle of electrochemically assisted leaching being applied to recover a broader set of critical and valuable metals from a range of primary and secondary feedstocks. The present study serves to assist in the development of more resilient supply chains for critical minerals.

■ ASSOCIATED CONTENT

Supporting Information

The Supporting Information is available free of charge at https://pubs.acs.org/doi/10.1021/acsomega.4c07361.

Electrochemically assisted leaching, Box-Behnken experimental design, and analyses of response surface methodology results including development of second-order regression modeling (PDF)

■ AUTHOR INFORMATION

Corresponding Author

Meng Shi − *Critical Materials Innovation Hub (CMI), Energy and Environment Science and Technology (EES&T) Division, Idaho National Laboratory, Idaho Falls, Idaho 83415, United States;* orcid.org/0000-0002-0892-4828; Phone: +1-208-526-3781; Email: Meng.Shi@inl.gov

Authors

Reyixiati Repukaiti − *Critical Materials Innovation Hub (CMI), Energy and Environment Science and Technology (EES&T) Division, Idaho National Laboratory, Idaho Falls, Idaho 83415, United States*

Arindam Mukhopadhyay − *Critical Materials Innovation Hub (CMI), Energy and Environment Science and Technology (EES&T) Division, Idaho National Laboratory, Idaho Falls, Idaho 83415, United States;* orcid.org/0000-0002-0620-4157

Luis A. Diaz − *Critical Materials Innovation Hub (CMI), Energy and Environment Science and Technology (EES&T) Division, Idaho National Laboratory, Idaho Falls, Idaho 83415, United States;* orcid.org/0000-0003-4895-464X

Caleb C. Stetson − *Critical Materials Innovation Hub (CMI), Energy and Environment Science and Technology (EES&T) Division, Idaho National Laboratory, Idaho Falls, Idaho 83415, United States;* orcid.org/0000-0003-0729-1261

Nighat A. Chowdhury − *Critical Materials Innovation Hub (CMI), Department of Systems and Industrial Engineering, University of Arizona, Tucson, Arizona 85721, United States*

Hongyue Jin − *Critical Materials Innovation Hub (CMI), Department of Systems and Industrial Engineering, University of Arizona, Tucson, Arizona 85721, United States*

Complete contact information is available at: https://pubs.acs.org/10.1021/acsomega.4c07361

Author Contributions

The manuscript was written through contributions of all authors. All authors have given approval to the final version of the manuscript.

Notes

The authors declare no competing financial interest.

■ ACKNOWLEDGMENTS

This work was supported by the Critical Materials Innovation Hub, an Energy Innovation Hub funded by the US Department of Energy's Office of Energy Efficiency and Renewable Energy's (EERE) Advanced Materials and Manufacturing Technologies Office (AMMTO). Work at Idaho National Laboratory was conducted under DOE contract E-AC07-05ID14517. Work at the University of Arizona was conducted under subcontract number SC-21-556 with the Ames National Laboratory. The authors want to acknowledge the technical support and materials provided Michael Rodriguez at Jervois Global.

■ REFERENCES

(1) United Nations *Net-Zero Coalition*. United Nations, 2015. https://www.un.org/en/climatechange/net-zero-coalition.

(2) International Energy Agency *Global EV Outlook 2023: Trends in Batteries*. International Energy Agency, 2023. https://www.iea.org/reports/global-ev-outlook-2023/trends-in-batteries.

(3) Colato, J.; Ice, L. Charging into the future: the transition to electric vehicles. In *Beyond the Numbers: Employment & Unemployment*; U.S. Bureau of Labor Statistics, 2023.
(4) Sun, X.; Hao, H.; Hartmann, P.; Liu, Z.; Zhao, F. Supply risks of lithium-ion battery materials: An entire supply chain estimation. *Materials Today Energy* **2019**, *14*, 100347.
(5) Miatto, A.; Graedel, T. E. U. S. cobalt scenario analysis to mid-century: Import dependency or marketable commodity? *Resour. Conserv. Recycl.* **2023**, *17*, 200134.
(6) Markets, R. a. *Market value of cobalt worldwide from 2021 to 2023, with a forecast for 2030*; 2023.
(7) Zheng, C.; Jiang, K.; Cao, Z.; Wang, H.; Liu, S.; Waters, K. E.; Ma, H. Pressure leaching behaviors of copper-cobalt sulfide concentrate from Congo. *Sep. Purif. Technol.* **2023**, *309*, 123010.
(8) Crundwell, F. K.; du Preez, N. B.; Knights, B. D. H. Production of cobalt from copper-cobalt ores on the African Copperbelt − An overview. *Miner. Eng.* **2020**, *156*, 106450.
(9) Bookstrom, A. A. The Idaho cobalt belt. In *Northwest Geology*; USGS Publications Warehouse, 2013; Vol. *42*, pp 149−162.
(10) Jervois *Updated RAM resource offers opportunity to extend ICO mine life*, 2023.
(11) Sletten, M.; Zelligan, S.; Frost, D.; Yugo, N.; Charbonneau, C.; Cameron, D. P. *Idaho Cobalt Operations Form 43-101F1 Technical Report Feasibility Study*; Jervois, 2020.
(12) Wang, G. X.; Chandra, D.; Fuerstenau, M. C. Oxidation of cobaltite: Part I. process mineralogy. *Metall. Mater. Trans. B* **1995**, *26* (3), 517−522.
(13) *Arsenic, The World Health Organization*; The World Health Organization, 2022. https://www.who.int/news-room/fact-sheets/detail/arsenic.
(14) Chung, J. Y.; Yu, S. D.; Hong, Y. S. Environmental source of arsenic exposure. *J. Prev Med. Public Health* **2014**, *47* (5), 253−257.
(15) Hughes, M. F. Arsenic toxicity and potential mechanisms of action. *Toxicol. Lett.* **2002**, *133* (1), 1−16.
(16) Saha, J. C.; Dikshit, A. K.; Bandyopadhyay, M.; Saha, K. C. A Review of Arsenic Poisoning and its Effects on Human Health. *Crit. Rev. Environ. Sci. Technol.* **1999**, *29* (3), 281−313.
(17) Yu, M.; Zhang, Y.; Fang, M.; Jehan, S.; Zhou, W. Current Advances of Nanomedicines Delivering Arsenic Trioxide for Enhanced Tumor Therapy. *Pharmaceutics* **2022**, *14* (4), 743.
(18) Komorowicz, I.; Hanć, A. Can arsenic do anything good? Arsenic nanodrugs in the fight against cancer − last decade review. *Talanta* **2024**, *276*, 126240.
(19) Postek, W. B.; Rutkowska, I. A.; Cox, J. A.; Kulesza, P. J. Electrocatalytic effects during redox reactions of arsenic at platinum nanoparticles in acid medium: Possibility of preconcentration, electroactive film formation, and detection of As(III) and As(V). *Electrochim. Acta* **2019**, *319*, 499−510.
(20) Chen, W.-C.; Wang, X.-L.; Qin, C.; Shao, K.-Z.; Su, Z.-M.; Wang, E.-B. A carbon-free polyoxometalate molecular catalyst with a cobalt−arsenic core for visible light-driven water oxidation. *Chem. Commun.* **2016**, *52* (61), 9514−9517.
(21) Crundwell, F. K.; Moats, M. S.; Ramachandran, V.; Robinson, T. G.; Davenport, W. G. *Extractive Metallurgy of Nickel, Cobalt and Platinum Group Metals*; Elsevier, 2011..
(22) Dehaine, Q.; Tijsseling, L. T.; Glass, H. J.; Törmänen, T.; Butcher, A. R. Geometallurgy of cobalt ores: A review. *Miner. Eng.* **2021**, *160*, 106656.
(23) Mwema, M. D. M. M.; Kafumbila, K. Use of sulphur dioxide as reducing agent in cobalt leaching at Shituru hydrometallurgical plant. *J. South. Afr. Inst. Min. Metall.* **2002**, *102* (1), 1−4.
(24) Senanayake, G.; Das, G. K.; de Lange, A.; Li, J.; Robinson, D. J. Reductive atmospheric acid leaching of lateritic smectite/nontronite ores in H2SO4/Cu(II)/SO2 solutions. *Hydrometallurgy* **2015**, *152*, 44−54.
(25) Das, G. K.; de Lange, J. A. B. Reductive atmospheric acid leaching of West Australian smectitic nickel laterite in the presence of sulphur dioxide and copper(II). *Hydrometallurgy* **2011**, *105* (3), 264−269.
(26) Shen, Y. F.; Xue, W. Y.; Li, W.; Tang, Y. L. Selective recovery of nickel and cobalt from cobalt-enriched Ni−Cu matte by two-stage counter-current leaching. *Sep. Purif. Technol.* **2008**, *60* (2), 113−119.
(27) Kaya, S.; Topkaya, Y. A. High pressure acid leaching of a refractory lateritic nickel ore. *Miner. Eng.* **2011**, *24* (11), 1188−1197.
(28) Whittington, B. I.; Muir, D. Pressure Acid Leaching of Nickel Laterites: A Review. *Miner. Process. Extr. Metall. Rev.* **2000**, *21* (6), 527−599.
(29) Stanković, S.; Kamberović, Z.; Friedrich, B.; Stopić, S. R.; Sokić, M.; Marković, B.; Schippers, A. Options for Hydrometallurgical Treatment of Ni-Co Lateritic Ores for Sustainable Supply of Nickel and Cobalt for European Battery Industry from South-Eastern Europe and Turkey. *Metals* **2022**, *12* (5), 807.
(30) Zhang, R.; Hedrich, S.; Römer, F.; Goldmann, D.; Schippers, A. Bioleaching of cobalt from Cu/Co-rich sulfidic mine tailings from the polymetallic Rammelsberg mine, Germany. *Hydrometallurgy* **2020**, *197*, 105443.
(31) Abdollahi, H.; Saneie, R.; Shafaei, S. Z.; Mirmohammadi, M.; Mohammadzadeh, A.; Tuovinen, O. H. Bioleaching of cobalt from magnetite-rich cobaltite-bearing ore. *Hydrometallurgy* **2021**, *204*, 105727.
(32) Johnson, D. B.; Dybowska, A.; Schofield, P. F.; Herrington, R. J.; Smith, S. L.; Santos, A. L. Bioleaching of arsenic-rich cobalt mineral resources, and evidence for concurrent biomineralisation of scorodite during oxidative bio-processing of skutterudite. *Hydrometallurgy* **2020**, *195*, 105395.
(33) Ntakamutshi, P. T.; Kime, M.-B.; Mwema, M. E.; Ngenda, B. R.; Kaniki, T. A. Agitation and column leaching studies of oxidised copper-cobalt ores under reducing conditions. *Miner. Eng.* **2017**, *111*, 47−54.
(34) Santoro, L.; Tshipeng, S.; Pirard, E.; Bouzahzah, H.; Kaniki, A.; Herrington, R. Mineralogical reconciliation of cobalt recovery from the acid leaching of oxide ores from five deposits in Katanga (DRC). *Miner. Eng.* **2019**, *137*, 277−289.
(35) Astuti, W.; Nurjaman, F.; Rofiek Mufakhir, F.; Sumardi, S.; Avista, D.; Cleary Wanta, K.; Tri Bayu Murti Petrus, H. A novel method: Nickel and cobalt extraction from citric acid leaching solution of nickel laterite ores using oxalate precipitation. *Miner. Eng.* **2023**, *191*, 107982.
(36) Zhang, M.; Zhu, G.; Zhao, Y.; Feng, X. A study of recovery of copper and cobalt from copper−cobalt oxide ores by ammonium salt roasting. *Hydrometallurgy* **2012**, *129−130*, 140−144.
(37) Tian, L.; Gong, A.; Wu, X.; Yu, X.; Xu, Z.; Chen, L. Process and kinetics of the selective extraction of cobalt from high-silicon low-grade cobalt ores using ammonia leaching. *Int. J. Miner., Metall. Mater.* **2022**, *29* (2), 218−227.
(38) Drahota, P.; Filippi, M. Secondary arsenic minerals in the environment: A review. *Environ. Int.* **2009**, *35* (8), 1243−1255.
(39) Nazari, A. M.; Radzinski, R.; Ghahreman, A. Review of arsenic metallurgy: Treatment of arsenical minerals and the immobilization of arsenic. *Hydrometallurgy* **2017**, *174*, 258−281.
(40) Dunne, R. C.; Kawatra, S. K.; Young, C. A. *SME Mineral Processing & Extractive Metallurgy Handbook*; Society for Mining, Metallurgy, and Exploration (SME), 2019.
(41) Twidwell, L. *Treatment of Arsenic-Bearing Minerals and Fixation of Recovered Arsenic Products: An Updated Review*; Montana Tech Library, 2018.
(42) Agency, U. S. E. P. *SW-846 Test Method 1311: Toxicity Characteristic Leaching Procedure*, 1992.
(43) Binnemans, K.; Jones, P. T. The Twelve Principles of Circular Hydrometallurgy. *J. Sustain. Metall.* **2023**, *9* (1), 1−25.
(44) Diaz, L. A.; Clark, G. G.; Lister, T. E. Optimization of the Electrochemical Extraction and Recovery of Metals from Electronic Waste Using Response Surface Methodology. *Ind. Eng. Chem. Res.* **2017**, *56*, 7516−7524.
(45) Diaz, L. A.; Strauss, M. L.; Adhikari, B.; Klaehn, J. R.; McNally, J. S.; Lister, T. E. Electrochemical-assisted Leaching of Active Materials from Lithium Ion Batteries. *Resour. Conserv. Recycl.* **2020**, *161*, 104900.

https://doi.org/10.1021/acsomega.4c07361
ACS Omega 2025, 10, 655−664

(46) Shi, M.; Diaz, L. A.; Klaehn, J. R.; Wilson, A. D.; Lister, T. E. Li2CO3 Recovery through a Carbon-negative Electrodialysis of Lithium-ion Battery Leachates. *ACS Sustain. Chem. Eng.* **2022**, *10*, 11773−11781.
(47) Adhikari, B.; Chowdhury, N. A.; Diaz, L. A.; Jin, H.; Saha, A. K.; Shi, M.; Klaehn, J. R.; Lister, T. E. Electrochemical leaching of critical materials from lithium-ion batteries: A comparative life cycle assessment. *Resour., Conserv. Recycl.* **2023**, *193*, 106973.
(48) Ma, B.; Wang, C.; Yang, W.; Yin, F.; Chen, Y. Screening and reduction roasting of limonitic laterite and ammonia-carbonate leaching of nickel−cobalt to produce a high-grade iron concentrate. *Miner. Eng.* **2013**, *50*−*51*, 106−113.
(49) Dong, Z.; Jiang, T.; Xu, B.; Zhang, B.; Liu, G.; Li, Q.; Yang, Y. A systematic and comparative study of copper, nickel and cobalt-ammonia catalyzed thiosulfate processes for eco-friendly and efficient gold extraction from an oxide gold concentrate. *Sep. Purif. Technol.* **2021**, *272*, 118929.
(50) de Oca, D. M. M.; Shi, M.; Diaz, L. A.; Lister, T. E. Electrochemical leaching of spent LIBs: Kinetics, novel reactor, and modeling. *Sustainable Mater. Technol.* **2024**, *40*, No. e00898.
(51) Shi, M.; Reich, S. M.; Verma, A.; Klaehn, J. R.; Diaz, L. A.; Lister, T. E. *Extraction of Nickel from Recycled Lithium-Ion Batteries*; Springer International Publishing, 2022; pp 163−172.
(52) Otgon, N.; Zhang, G.; Zhang, K.; Yang, C. Removal and fixation of arsenic by forming a complex precipitate containing scorodite and ferrihydrite. *Hydrometallurgy* **2019**, *186*, 58−65.
(53) O'Day, P. A.; Vlassopoulos, D.; Root, R.; Rivera, N. The influence of sulfur and iron on dissolved arsenic concentrations in the shallow subsurface under changing redox conditions. *Proc. Natl. Acad. Sci. U.S.A.* **2004**, *101* (38), 13703−13708.
(54) Filippou, D.; Demopoulos, G. P. Arsenic immobilization by controlled scorodite precipitation. *JOM* **1997**, *49* (12), 52−55.
(55) Ma, X.; Gomez, M. A.; Yuan, Z.; Zhang, G.; Wang, S.; Li, S.; Yao, S.; Wang, X.; Jia, Y. A novel method for preparing an As(V) solution for scorodite synthesis from an arsenic sulphide residue in a Pb refinery. *Hydrometallurgy* **2019**, *183*, 1−8.
(56) Bard, A. J.; Faulkner, L. R.; White, H. S. *Electrochemical methods: fundamentals and applications*; John Wiley & Sons, 2022.
(57) Taylor, P. R.; Vanderloop, J. P. An investigation into the leaching kinetics of cobaltite ore with ferric sulfate solutions. *Metall. Trans. B* **1980**, *11* (1), 83−88.
(58) Qi, Y.; Li, D.; Zhang, S.; Li, F.; Hua, T. Electrochemical filtration for drinking water purification: A review on membrane materials, mechanisms and roles. *J. Environ. Sci.* **2024**, *141*, 102.
(59) Clapp, M.; Zalitis, C. M.; Ryan, M. Perspectives on current and future iridium demand and iridium oxide catalysts for PEM water electrolysis. *Catal. Today* **2023**, *420*, 114140.
(60) Wang, Y.; Chang, X.; Chen, M.; Qin, W.; Han, J. Effective extraction of nickel and cobalt from sintered nickel alloy via reduction roasting and leaching. *Miner. Eng.* **2023**, *203*, 108336.
(61) Zhou, L.; Yang, J.; Kang, S.; Wang, X.; Yu, H.; Wan, Y. Enhancing leaching efficiency of ion adsorption rare earths by ameliorating mass transfer effect of rare earth ions by applying an electric field. *J. Rare Earths* **2024**, *42*, 172.
(62) Moro, K.; Haubrich, F.; Martin, M.; Grimmer, M.; Hoth, N.; Schippers, A. Reductive leaching behaviour of manganese and cobalt phases in laterite and manganese ores. *Hydrometallurgy* **2023**, *220*, 106101.
(63) Sethurajan, M.; Shirodker, M. G. P.; Rene, E. R.; van Hullebusch, E. D. Hydrometallurgical leaching and recovery of cobalt from lithium ion battery. *Environ. Technol. Innovation* **2022**, *28*, 102915.
(64) Feng, Z.; Gupta, G.; Mamlouk, M. A review of anion exchange membranes prepared via Friedel-Crafts reaction for fuel cell and water electrolysis. *Int. J. Hydrogen Energy* **2023**, *48* (66), 25830−25858.

https://doi.org/10.1021/acsomega.4c07361
ACS Omega 2025, 10, 655−664